Effect of thermal aging on the room temperature tensile properties of AISI type 316LN stainless steel

P. Shankar [a], H. Shaikh [a], S. Sivakumar [b], S. Venugopal [a], D. Sundararaman [a], H.S. Khatak [a,*]

[a] *Metallurgy and Materials Group, Indira Gandhi Centre for Atomic Research, Kalpakkam, Tamil Nadu 603 102, India*
[b] *Department of Metallurgical Engineering, Regional Engineering College, Tiruchirappalli 620 015, India*

Abstract

Round tensile specimens of AISI type 316LN stainless steel, thermally aged at 1123 K for 0, 2, 10, 25, 100, 500 and 1000 h, were tested for tensile properties at room temperature at a strain rate of 7.7×10^{-3} s^{-1}. The changes in tensile properties were correlated to the transmission electron microscopic studies. The various stages of nitrogen repartitioning including Cr–N cluster formation, intragranular and subsequent cellular precipitation of Cr$_2$N were found to have a strong influence on the yield strength (YS) and ductility of the material. However, the changes in ultimate tensile strength (UTS) with aging were negligible. The results of electrochemical extraction of secondary phases clearly indicated a two-slope behavior. X-ray diffraction analysis of electrochemically extracted residue suggested that the initial smaller sloped line corresponded to the precipitation of the Cr$_2$N phase while the line with larger slope at longer aging time corresponded to the domination of chi phase precipitation. © 1999 Elsevier Science B.V. All rights reserved.

1. Introduction

Austenitic stainless steels are the most common materials used for a variety of applications ranging from the paper and pulp industry to the chemical, petrochemical and nuclear industries. Sensitization is a common problem encountered with these types of stainless steels. In fact, failure of coolant channels in Boiling Water Reactors was attributed to intergranular stress corrosion cracking arising from sensitization. The problem of sensitization could be overcome by using low carbon stainless steels. To compensate for the associated loss in strength, nitrogen is added to these stainless steels. Nitrogen alloyed austenitic stainless steels find extensive application as structural materials in nuclear reactors. Nuclear grade AISI type 316LN austenitic stainless steel containing about 800 ppm of nitrogen is the candidate structural material for fast breeder reactors. It is used in many structural components like main vessel, safety vessel, inner vessel, auxillary grid plate,

fuel transfer machines, intermediate heat exchangers, core support structures, etc., because of its superior strength, better corrosion resistance, good weldability and adequate mechanical properties at high temperatures, as compared to AISI type 316 stainless steel.

Nitrogen not only improves the intergranular stress corrosion cracking resistance, but also plays a key role in improving pitting corrosion resistance and in enhancing several other mechanical properties. Nitrogen is the most effective solid solution strengthener in austenite [1]. Nitrogen in solid solution has a remarkable influence on tensile and creep strength of the material. Increase in creep strength and decrease in minimum creep rate with nitrogen addition has been attributed either to solid solution strengthening or to the presence of short-range ordered zones [2]. The effect of dissolved nitrogen has been reported to be much more pronounced on UTS than on YS. Addition of nitrogen increases the work hardening rate, resulting in more uniform strain prior to plastic instability. This results in increase of total ductility before failure [3]. Addition of nitrogen to austenitic steels results in increase in both the thermal and athermal components of flow stress [4]. The thermal

---

* Corresponding author.

component of flow stress is directly proportional to the square root of nitrogen concentration. This is attributed primarily to the interaction of dislocations with short-range ordered zones or Cr–N clusters in the austenite matrix. Since the formation of the nitrogen-rich clusters are thermally activated processes involving the diffusion of nitrogen atoms, the square root dependence of the thermal component on nitrogen concentration can be understood. In contrast, the athermal component of flow stress varies linearly with the nitrogen concentration [5]. Nitrogen also has a beneficial effect on the low cycle fatigue behavior of austenitic stainless steels, both at room temperature as well as at high temperatures. The substantial increase in fatigue life with nitrogen addition has been attributed to its effect in enhancing the coplanar slip. Coplanar slip can be promoted by either (a) decrease in stacking fault energy with nitrogen addition, (b) presence of Cr–N complexes, (c) presence of short-range ordered zones in the austenite matrix [6].

It is, therefore, obvious that the microstructure has a dominating influence on the mechanical properties of nitrogen alloyed austenitic stainless steels. The emphasis of this paper is to correlate the room temperature tensile properties with the microstructure of AISI type 316LN stainless steels aged at 1123 K for various time durations.

2. Experimental procedures

The composition of type 316LN stainless steel used in the present study is given in Table 1. The as-received stainless steel plates were solution annealed (SA) at a temperature of 1323 K in a vacuum of about 10^{-5} Torr. The SA plates were then thermally aged at 1123 K for various time durations of 2, 10, 25, 100, 500 and 1000 h.

Round tension specimens, shown in Fig. 1, were machined from the solution annealed and aged stainless steel plates. Tensile tests were carried out using an IN-STRON 1195 universal testing machine at an initial strain rate of 7.7×10^{-3} s^{-1} at room temperature. Two specimens were tested for each thermally aged condition and their average was taken as the representative value. The scatter associated with each data is also represented in the Figs. 2–4, showing the effect of aging on the YS, UTS and ductility, respectively.

After etching AISI type 316LN stainless steel specimens in 10% (by weight) ammonium persulfate solution, metallographic examinations were carried out in a Reichert Model MeF2 optical microscope to ascertain the
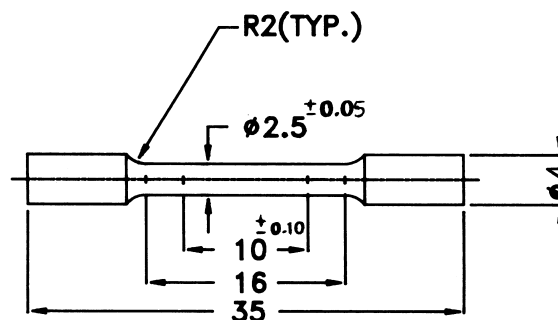

Fig. 1. Schematic of the round tension specimens used in the present study.

changes in microstructures and grain size from aging. Transmission electron microscopic (TEM) studies were carried out to ascertain the precipitation sequence. The amount of precipitates in the aged specimens was determined after electrochemically extracting them in a solution containing 10% HCl in methanol at a potential of 1.5 V with respect to the platinum electrode. At this potential, austenite dissolves leaving behind a residue of these precipitates. Weighing the specimen before and after extraction and weighing the precipitate content, after centrifuging and drying, would yield the fraction of precipitates in the stainless steel. X-ray diffraction analysis of the extracted precipitates was carried out to identify them.

3. Results

The load versus elongation data, obtained from various tensile tests, were analyzed to determine the YS, UTS and ductility. Figs. 2 and 3 show the variations in YS and UTS with aging time, respectively. Fig. 4(a) shows the influence of aging on the reduction in area (RA), while 4(b) shows the dependence of total elongation on the aging condition. YS was found to change substantially on aging. An increase of 25 MPa was observed in YS on aging for 2 h and a subsequent decrease of about 80 MPa was noticed on aging up to 10 h. Continued aging for 100 h caused an increase in YS by about 40 MPa. Thereafter, there was a continuous decrease in YS on aging the material up to 1000 h. Thermal aging had a similar influence on UTS also, although to a lesser extent as compared to the dependence of YS. The changes in UTS were within about ±2.5% of the value of SA material. RA of the material increased by

Table 1
Composition in weight percent of the AISI type 316LN stainless steel

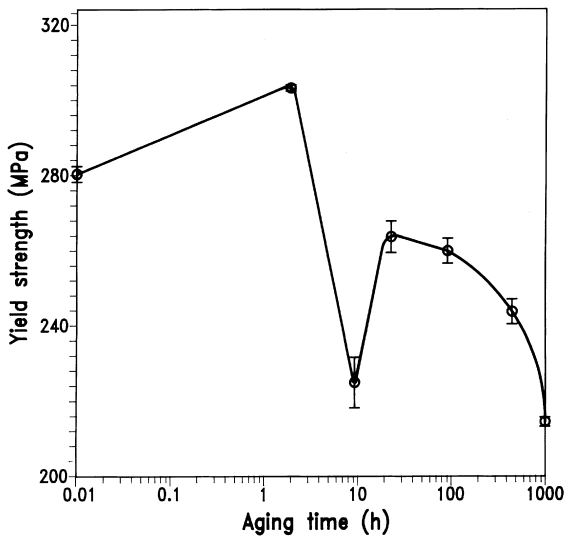| Element	C	Mn	Ni	Cr	Mo	N	S	P
(% wt)	0.021	1.74	12	17	2.4	0.078	0.002	0.023

Fig. 2. Plot showing the variation of YS with aging at 1123 K.

Fig. 3. Plot showing the variation of UTS with aging at 1123 K.

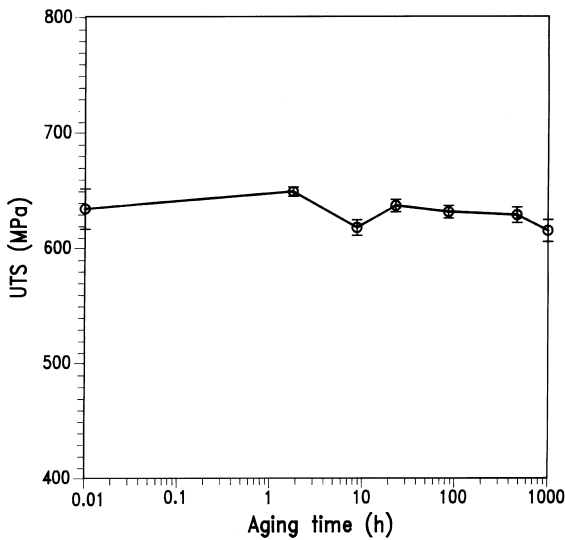Fig. 4. (a) Plot showing the variation in RA with aging at 1123 K. (b) Plot showing the variation in total elongation with aging at 1123 K.

about 15% on aging to 10 h. Further aging led to a continuous reduction in RA up to about 20% (vis-à-vis 10 h aged material) on aging for 1000 h. The variations in total elongation (TE) as a function of aging time also showed a trend similar to RA, although to a lesser magnitude.

Fig. 5 shows the characteristic two-slope behavior between the amount of extracted precipitates and aging time. X-ray diffraction analysis of these precipitates revealed the presence of $M_{23}C_6$, chi and Cr_2N phases in specimens aged for 25 h and above. Electrochemical extraction of solution annealed samples and those aged up to 10 h did not yield a significant amount of pre-
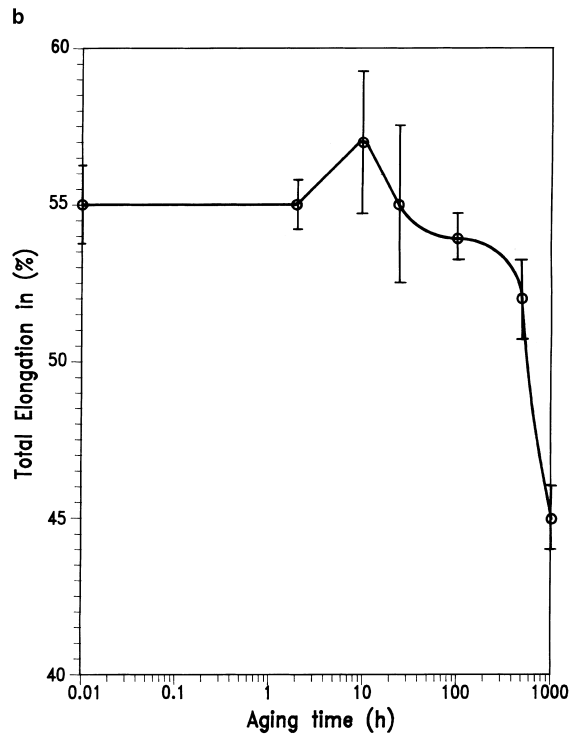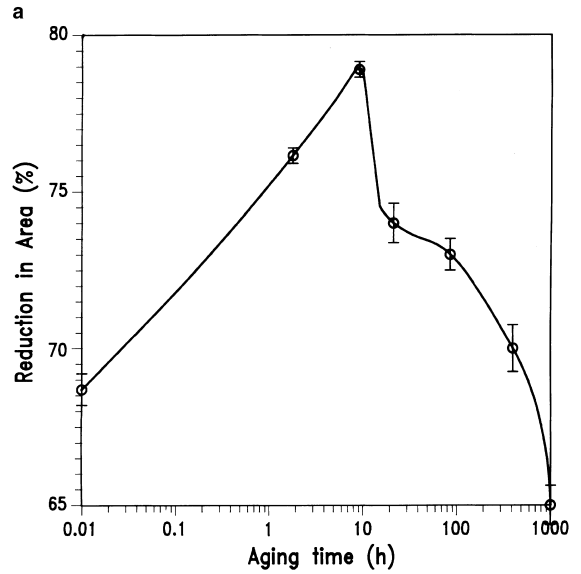
cipitates. By comparing the ratio of peak intensities from two different phases, (Table 2), the relative changes in their volume fraction on aging was estimated. Cr_2N precipitation was very dominant on aging up to 25 h. Thereafter, the fraction of Cr_2N precipitates in the
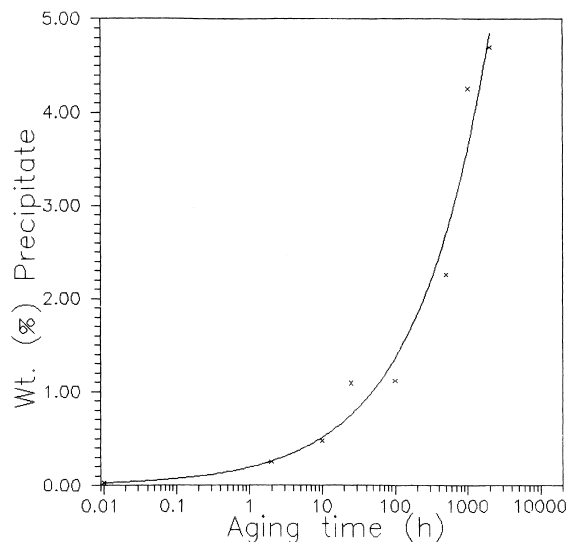
Fig. 5. Figure showing the dependence of weight percentage of extracted precipitates on the aging time.

Table 2
Ratio of XRD peak intensities for two different phases as a function of aging time

Aging time (h)	25	100	500	1000	2000
$Cr_2N/M_{23}C_6$	3.098	2.74	2.0664	1.9388	1.675
Cr_2N/chi	6.73	4.27	2.645	2.11	0.8272

electrochemical residue decreased with increasing aging time in comparison to the fraction of $M_{23}C_6$ and chi phases. The increase in amount of chi phase in the electrochemical residue was significantly more than the increase in $M_{23}C_6$ with increasing aging time. From the XRD results, it can be conceived that the initial lower slope corresponds to Cr_2N precipitation while the higher slope at longer aging times corresponds to chi phase precipitation.

4. Discussion

Optical microscopy examination showed no significant changes in grain size of the material on aging. All the observed changes in the tensile behavior can therefore be attributed only to changes in the microstructural state of the material. The changes in tensile properties are discussed with respect to changes in the morphology and distribution of the Cr_2N phase and the precipitation of the chi phase. Shankar et al. [7–9] had earlier characterized the various stages of microstructural evolution of AISI type 316LN stainless steel on thermal aging at 1123 K by TEM. They stated that nitrogen was present in a supersaturated state in the solution-annealed con-

dition. Thermal aging had a remarkable effect on microchemical repartitioning of nitrogen into more stable sites and configurations. The high affinity of nitrogen for chromium results in a significant driving force for maximization of Cr–N interactions in the matrix on aging, in contrast to the random distribution of chromium and nitrogen in the solution annealed state. Thermodynamic correlation by Grujicic et al. [4], had shown that there was more than 80% probability of nitrogen atoms to be surrounded by three or more chromium atoms in Wagner's cell model. Therefore, during the early stages of aging, there was a tendency for chromium and nitrogen atoms to bond with each other and to form clusters, thus reducing the free energy of the system. The number density of such clusters was seen to be maximum on aging for 10 h, based on both CTEM and HREM investigations [7]. Cr–N rich fcc clusters were observed up to 25 h of aging. However the formation of such clusters is obviously a kinetically constrained process, controlled predominantly by the slower diffusing chromium atoms. Therefore, during the very early stages of aging, not all nitrogen would be bonded to chromium atoms. The nitrogen atoms can alternatively bind with dislocations which is also another energy minimizing process. Dislocations with oscillatory contrast were observed in specimens aged for 2 h when imaged with $[0\ 1\ 1]_g$ as zone axis and $(1\ 1\ 1)_g$ as the operating reflection, as is shown in Fig. 6. The oscillatory contrast remained even on varying the deviation parameter (s_g) over a range by tilting the specimen about the zone axis. Also, similar dislocation contrast was not observed in solution annealed specimens and those aged for more than 10 h. All this probably suggests that the oscillatory dislocation contrast seen in specimens aged for 2 h is due to segregation of nitrogen atoms to dislocations. Aging for and beyond 25 h was found to
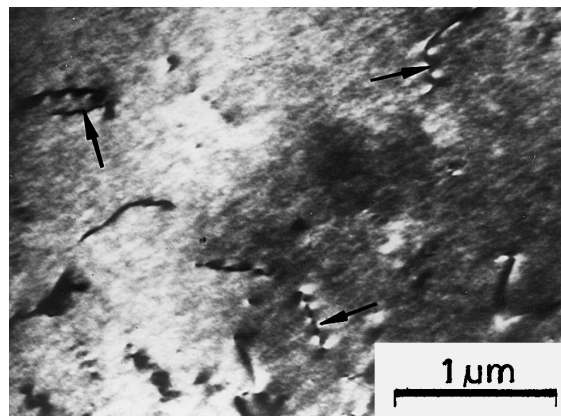

Fig. 6. TEM micrograph showing oscillatory contrast of dislocations imaged with $(1\ 1\ 1)_g$ as operating reflection and with $[0\ 1\ 1]_g$ as zone axis in a specimen aged for 2 h.
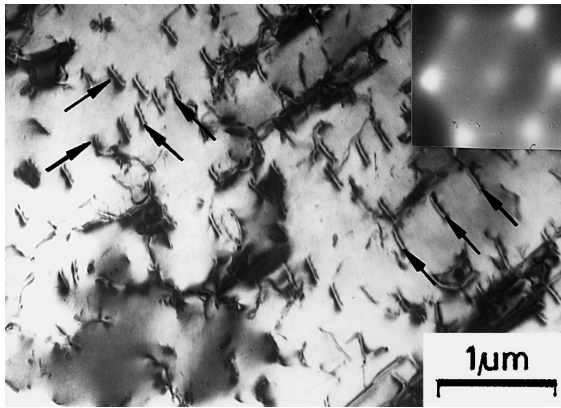
Fig. 7. Formation of dislocation pairs on aging, found to be associated with the precipitation of intragranular ordered Cr_2N phase. Inset shows the $[0\,0\,0\,1]_{Cr_2N}$ SAD pattern.

result in the formation of dislocation pairs (Fig. 7). SAD patterns from regions enclosing such dislocation pairs resulted in Cr_2N reciprocal lattice sections, thereby unambiguously concluding the association of dislocation pairs with precipitation of the hcp interstitially ordered Cr_2N phase [8]. The $[0\,0\,0\,1]$ SAD pattern of Cr_2N is provided as inset to Fig. 7. Continued aging beyond 500 h resulted in intergranular precipitation of Cr_2N (Fig. 8). Thus, it is obvious that the microstructural state of the system is sensitive to the thermal history. Hence, it can be concluded that the following microstructural changes occur: (i) formation of Cr–N clusters, (ii) intragranular Cr_2N precipitation, (iii) intergranular Cr_2N precipitation, (iv) depletion of solid solution strengtheners like Cr, Mo, C, N, associated with copious precipitation of chi and $M_{23}C_6$ phases.

The increase in YS on aging the steel for 2 h can be explained based on pinning of dislocations by nitrogen. Formation of Cr–N clusters was in its infancy after 2 h
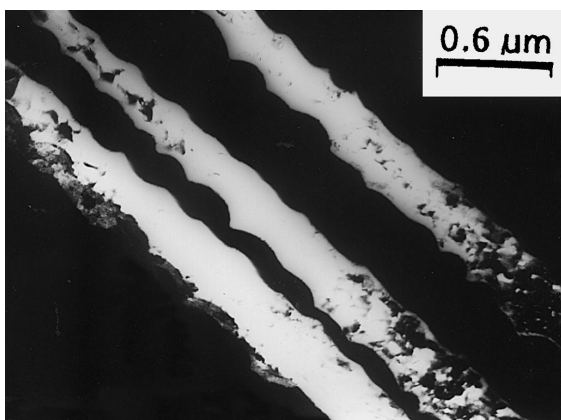

Fig. 8. Cellular precipitation of Cr_2N on aging beyond 500 h.

of aging, during which not all nitrogen atoms were bonded with chromium, due to the much slower diffusion kinetics of the latter. The remaining nitrogen atoms tend to segregate to dislocations and thereby minimize the strain energy of austenite. Also, Gavriljuk et al. [10] have shown by the amplitude dependent internal friction (ADIF) method, that nitrogen has a stronger pinning effect on dislocations than carbon in the austenite matrix. Thus, segregation of nitrogen atoms to dislocations would necessitate larger stresses to move them, thereby increasing the YS.

On aging for 10 h, almost all the nitrogen atoms were bonded with chromium atoms as Cr–N rich clusters. These clusters are generally known to act as barriers for dislocation motion. Because of the very small volume fraction of clusters in a 0.08% N steel used in the present study, most dislocations do not encounter these obstacles during deformation. Hence, the matrix effect predominantly governs the tensile behavior under such conditions. The effect of depletion of solid solution strengtheners like nitrogen from matrix on decreasing YS, overrides the positive contribution due to interaction of a small number of dislocations with clusters. This results in a remarkable decrease in proof stress on aging for 10 h. In a study on Fe–18% Cr–10% Ni steel, Reed [11] estimated that the addition of 1 wt% of nitrogen in the solid solution of austenite increases the YS of AISI type 316L stainless steel by about 710 MPa at 295 K. If it is assumed in the present study that all (0.08 wt%) nitrogen atoms come out of solution on aging at 10 h, then it should result in a decrease in yield strength by about 57 MPa as compared to the solution annealed condition. This is in good agreement with the observations in the present study, which shows a decrease in YS by about 56 MPa in an 10 h-aged sample as compared to the solution-annealed state.

Precipitation of very fine intragranular ordered Cr_2N, on aging for 25 h, resulted in increase in YS vis-à-vis specimens aged for 10 h. On aging beyond 25 hours, the precipitation of chi and $M_{23}C_6$ phases plays a role in determining the change in the YS of the material. Table 3 shows the changes in the amount of chi and $M_{23}C_6$ phases on aging AISI type 316LN stainless steel vis-à-vis the respective amounts in 25 h aged condition. The chi phase is a stable intermetallic compound containing iron, chromium and molybdenum [12]. It is a carbon dissolving compound of the type $M_{18}C$. It is seen from Table 3, that there is a substantial increase in the amount of $M_{23}C_6$ and chi phases on aging to and

Table 3
Ratio of XRD peak intensities from carbide and chi phases as a function of aging time

Aging time (h)	25	100	500	1000	2000
$M_{23}C_6$/chi	2.17	1.555	1.28	1.0888	0.494

beyond 100 h. The precipitation of these phases led to a significant decrease in solid solution strengtheners like Cr and Mo from the austenite matrix. The effect of dislocation pinning by the Cr_2N particles, which results in increase in YS, was more than overcome by the effect of depletion of solid solution strengtheners which decreases YS. This resulted in a decrease in YS beyond 25 h of aging. The changes in UTS, though following a similar behavior as YS, are within ±2.5% of the solution-annealed material. Hence, these changes in UTS can be neglected. The reason for negligible change in UTS is because the depletion of solute from matrix and dislocation–precipitate interactions have opposing tendencies on the UTS. Depletion of solid solution strengtheners, of which nitrogen is most potent, causes a decrease in UTS. But this decrease in UTS is offset and neutralized by the effect of precipitates–dislocation interaction which increase the UTS.

Thermal aging of AISI type 316LN stainless steel indicated an increase in ductility on aging up to 10 h. This is attributed to the softening of the austenite due to reduction of nitrogen in solid solution on formation of Cr–N clusters. Beyond 10 h of aging, ductility of the material decreases continuously up to 1000 h of aging. This decrease in ductility is attributed to the dominating effect of the interaction of dislocations with intragranular (at 25, 100 h) and cellular Cr_2N particles (at 500 and 1000 h) in reducing ductility. The hcp crystal structure of Cr_2N particles makes it less deformable as compared to the matrix, which has an fcc crystal structure. This leads to dislocation piling up at the particles during deformation, leading to stress concentration. The effect of triaxial state of stress in reducing ductility is well known [13]. Also, cellular precipitation is known to reduce the toughness of the materials. Since UTS is nearly constant, toughness decrease would mean a decrease in ductility. Thus cellular precipitation of Cr_2N also reduces ductility. Precipitation of the chi phase is not known to lead to reduction in creep ductility due to the good resistance to brittle microcracking of chi phases [12]. Hence, it is not expected to be detrimental to tensile ductility.

5. Conclusion

The following conclusions are drawn from the study on the effect of aging at 1123 K on the tensile properties of AISI type 316LN stainless steel:

1. Very short aging times resulted in an increase in YS as a consequence of nitrogen segregation to dislocation.

2. Formation of Cr–N clusters in specimens aged for 10 h is associated with a decrease in YS and increase in ductility, as a result of associated matrix softening.
3. Precipitation of intragranular coherent Cr_2N resulted in an increase in YS on aging for 25 h.
4. Substantial depletion of solid solution strengtheners mainly due to copious precipitation of chi phases at and beyond 100 h resulted in a remarkable decrease in yield strength.
5. The UTS of the material did not undergo any significant change on aging at 1123 K.
6. Depletion of solid solution strengtheners increased the tensile ductility on aging to 10 h, while intragranular and cellular precipitation of Cr_2N decreased the ductility thereafter.

References

[1] J.W. Simmons, Mater. Sci. Eng. 207A (1996) 159.
[2] L.A. Norstrom, Met. Sci. 11 (1977) 208.
[3] F.B. Pickering, Proceedings of the International Conference on High Nitrogen Steels, HNS88, Lille, France, The Institute of metals, May 1988, p. 10.
[4] M. Grujicic, J.O. Nilsson, W.S. Owen, T. Thorvaldsson, Proceedings of the International Conference on High Nitrogen Steels, HNS 88, Lille, France, The Institute of Metals, May 1988, p. 151.
[5] J. Rawers, M. Grujicic, Mater. Perform. 4 (1995) 697.
[6] S. Degalliax, J.I. Dickson, J. Foct, Proceedings of the International Conference on High Nitrogen Steels, HNS 88, Lille, France, The Institute of Metals, May 1998, p. 380.
[7] P. Shankar, D. Sundararaman S. Ranganathan, J. Nucl. Mater., accepted for publication.
[8] D. Sundararaman, P. Shankar, V.S. Raghunathan, Mater. Metall. Trans. 26A (1995) 1.
[9] P. Shankar, D. Sundararaman, V.S. Raghunathan, S. Ranganathan, Scripta Met. Mater. 31 (1994) 589.
[10] V.G. Gavriljuk, V.A. Duz', S.P. Jephimenko, Proceedings of the International Conference on High Nitrogen Steels, HNS 88, Lille, France, The Institute of Metals, May 1988, p. 447.
[11] R.P. Reed, J. Metals (1995) 16.
[12] J.K. Lai, J.R. Haigh, Weld. J. 58 (1979) 1s.
[13] G.E. Dieter, Mechanical Metallurgy, 4th ed., Mc-Graw Hill, New York, 1990, p. 263.